Chinese Chemical Letters 34 (2023) 108463

Contents lists available at ScienceDirect

Chinese Chemical Letters

journal homepage: www.elsevier.com/locate/cclet

Recent progress in MXenes incorporated into electrospun nanofibers for biomedical application: Study focusing from 2017 to 2022

Muheeb Rafiq[a], Sami-ullah Rather[b], Taha Umair Wani[a], Anjum Hamid Rather[a], Rumysa Saleem Khan[a], Anees Ellahi Khan[a], Ibtisam Hamid[a], Haseeb A. Khan[c], Abdullah S. Alhomida[c], Faheem A. Sheikh[a,*]

[a] *Nanostructured and Biomimetic Lab, Department of Nanotechnology, University of Kashmir Hazratbal, Jammu and Kashmir, Srinagar 190006, India*
[b] *Department of Chemical and Materials Engineering, King Abdulaziz University, Jeddah 21589, Saudi Arabia*
[c] *Research Chair for Biomedical Applications of Nanomaterials, Department of Biochemistry, College of Science, King Saud University, Riyadh 11451, Saudi Arabia*

ARTICLE INFO

Article history:
Received 31 January 2023
Revised 15 April 2023
Accepted 16 April 2023
Available online 18 April 2023

Keywords:
MXenes
Nanofibers
Tissue engineering
Antimicrobial
Electrospinning

ABSTRACT

After discovering a new class of two-dimensional (2D) material, *i.e.*, MXene, a further new scope, came into existence for researchers. Due to their remarkable physical, chemical, and biological properties, MXenes find their role in almost every research discipline. They have been used in biosensors, bioimaging, tissue engineering, drug delivery systems, and other areas. The MXenes can be functionalized with a wide range of atoms/molecules, making them diverse materials. Therefore, the potential of using MXenes in nanofibers can be much more than expected. In this review, we will understand the structure, synthesis, and general properties of MXenes. We will explain using MXenes while encasing them into nanofibers, providing their specific properties. For instance, MXenes-incorporated nanofibers are used in biomedical applications, including soft and hard-tissue engineering and delivery of antimicrobials. Furthermore, MXenes, when incorporated into nanofibers, are used in promoting cellular differentiation, wound healing, and neural tissue restoration, which are briefly discussed in this communication.

1. Introduction

Two-dimensional (2D) materials have remarkable and intriguing physiochemical properties because of their reduced dimensionality [1] and the quantum confinement effect [2]. Moreover, these materials are obtained by top-down exfoliation and/or bottom-up synthesis [3]. They include graphene [4], hexagonal boron nitride [5], and transition-metal dichalcogenides (MoS_2, WS_2, *etc.*) [6]. Further, single-element 2D materials such as phosphorene [7], silicene [8], borophene [9], and others have also been produced [10]. They became the central focus for material scientists since the discovery of 2D graphene [11]. For instance, graphene's high conductivity and in-plane rigidity have unanimously created interest in manufacturing flexible biomedical devices [12]. Similarly, MoS_2 has been used for its drug delivery and in developing the photothermal ability for different applications [13]. In the same context, borophene possesses a wide range of exciting properties, such as lightweight, excellent mechanical toughness, and remarkable superconducting capabilities, increasing its potential in electrical equipment for biomachines [14]. Similarly, black phosphorus nanosheets have distinct energy band configurations, size-dependent band gaps, and semiconductor properties, making them valid by generating electron-hole pairs when exposed to external ultrasounds [15]. However, many of these continue to be studied only for academic purposes; others have gained attention because of appealing features that have led to real-world applications [16]. These include the rapidly expanding class of 2D materials known as MXenes (pronounced "maxenes"), which consists of transition metal carbides and nitrides [17].

Among different nanomaterials, nanofibers are known for various biomedical applications [18]. Fabricating these materials involves numerous methods; however, electrospinning is preferred due to its versatility [19]. The process consists of electrifying a liquid droplet to create a jet, then stretching and elongating to form nanofiber [20]. Various polymeric solutions have been electrospun to obtain desired biocompatible materials, which find their applications, such as in bone [21] and neural [22,23] tissue engineering. Often these materials have been modified to improve their performance while incorporating other nanomaterials [24]. Biomaterials

* Corresponding author.
E-mail address: faheemnt@uok.edu.in (F.A. Sheikh).

https://doi.org/10.1016/j.cclet.2023.108463
1001-8417/

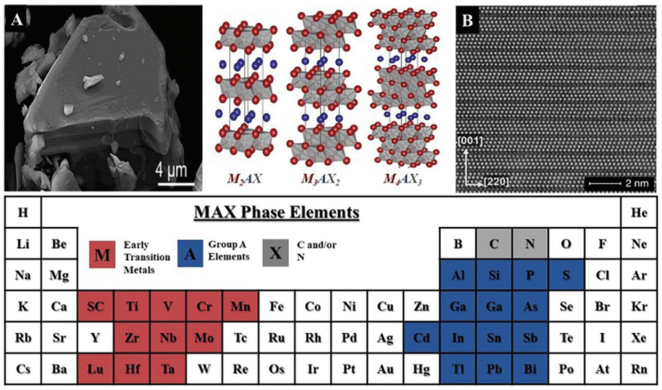

Fig. 1. Image showing SEM images of MAX phase material and elements that form these materials: (A) SEM of Ti_3AlC_2; (B) Images captured by high-resolution scanning transmission electron microscopy (HR-STEM) of the MAX phases of Ti_4SiC_3 (Ti atoms have brighter dots and Si atoms have darker spots). Reproduced with permission [43]. Copyright 2017, Elsevier B.V.; Reproduced with permission [44]. Copyright 2019, Elsevier B.V.; Reproduced with permission [45]. Copyright 2012, American Chemical Society.

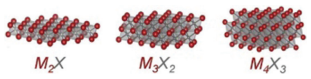

Fig. 2. Structure of single to multi-layer MXenes produced after etching. Reproduced with permission [44]. Copyright 2019, Elsevier B.V.

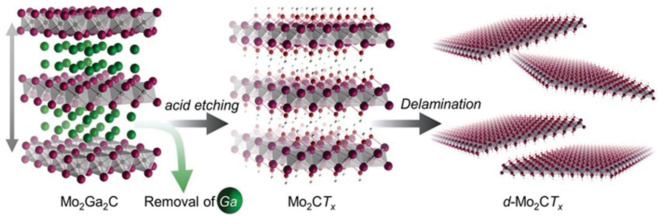

Fig. 3. Diagram demonstrating the creation and delamination of Mo_2CT_x. A solution comprising LiF and HCl was used to etch Mo_2Ga_2C powders, resulting in multi-layered Mo_2CT_x flakes with Li^+ ions in the interlayer space. Later on, deionized water is used to delaminate the Mo_2CT_x-Li. Reproduced with permission [47]. Copyright 2016, John Wiley & Sons.

are widely used for different applications for the betterment of life [25,26]. Likewise, graphene flakes were added to polyurethane to make them electroconductive; resultant substrates showed cell adhesion and proliferation [27]. Similarly, chitosan and carbon nanotubes have been incorporated into the polyurethane nanofibers, and the consequent material has been tested for cardiac tissue engineering [28]. On another note, chitosan and polydopamine have been assembled on silk fibroin nanofibers to make them antimicrobial and biocompatible [29]. In the above context, oils have also been added to nanofibers to make them useful for biological applications [30–32]. Nevertheless, after discovering MXenes, researchers are now trying to modify materials for better applications [33–35]. Owning to the potential application of MXenes in bioimaging [36], therapeutics [37], tissue engineering [38], antibacterial [39], and biosensors [40], attempts are made to encase these newly discovered materials in the nanofibers. Using different types of MXenes in polymeric nanofibers, they showed better results for antimicrobial, cell differentiation, wound healing, and other biomedical applications.

However, the potential use of MXenes to modify the nanofibers remains largely unexplored. It is noteworthy to mention these interventions have significantly marked their role in the biological application. Seeing the potential of this newly fabricated material, *i.e.*, MXenes and nanofibers, we summarize the current progress in the field. We have been focusing on MXenes, their structure, synthesis and properties to give an overall picture of this new material. However, this paper's central area of interest is the role of MXene-nanofiber composite for biomedical applications.

2. An outlook on MXenes: structure, synthesis, and properties

MXenes are one to few atomic layers thick with 2D arrangements that possess distinct properties from their 3D precursors, *i.e.*, MAX phase materials [41]. These materials are orderly arranged carbides and nitrides of ternary metals, where M is a transition metal (Mo, Zr, Cr, *etc.*), A represents group 13–16 elements (Al, Ge, Sn, *etc.*), and X can be either carbon, nitrogen, or a combination of the two. They are usually represented by $M_{n+1}AX_n$, where n ranges from 1 to 3. Here, the atoms are firmly packed as M layers, and the octahedral sites are filled by the X atoms, which are held together by the A atoms. This can be observed in Fig. 1. After the removal of A layer from MAX phase materials, a new class of 2D materials is obtained termed to MXenes (the suffix "ene" on these materials denotes that they are related to graphene) [42]. These materials are generally represented by $M_{n+1}X_nT_z$ ($n = 1–3$), where T_z means different termination sites, such as fluorine, hydroxyl, and/or oxygen atoms, and M is an early transition metal. At the same time, X is carbon and/or nitrogen, as shown in Fig. 2.

MXenes synthesis involves separating single or multiple atomic layers from MAX phase materials where the bonds between them are substantially weaker, later to be removed by chemical etching [46]. For this aim, aqueous fluoride-containing acids have been widely used as etchants [45]. This procedure involves stirring MAX phase powders with aqueous hydrogen fluoride at 25 °C for a predetermined time. The selective etching of the A layers of the MAX phase materials results in replacing the MX metallic bonds with weak surface termination bonds. Hydroxyl, fluoride, or oxygen is substituted for these metallic bonds between the MX layers. For instance, two Ga layers are etched in Mo_2Ga_2C for synthesizing Mo_2CT_x MXenes, as can be seen in Fig. 3 [47]. Furthermore, various etching techniques have been created and are summarized in Table 1.

The surface terminations of MXenes have a substantial impact to their mechanical characteristics; those with an O termination show high stiffness, but those with F or OH termination offer minimal elastic stiffness [60]. Notably, the surface-functionalized MXenes displayed more flexibility [61]. This property can attribute to the fabrication of flexible biosensors, which can be helpful in sending real-time electric signals upon physiological activity. Mostly they find their application as energy storage devices; they have been used in self-powered biomedical devices [62]. Moreover, they are ultrasensitive toward changes in the potential that can be used to detect specific biomarkers [63]. Concerning magnetic behavior, MXenes, like Ti_2N, Cr_2C and Ti_2C, are ferromagnetic, while oth-

Table 1
Various etching techniques are used in MXenes synthesis. Reproduced with permission [48]. Copyright 2019, Elsevier B.V.

Type of method	Etchant	Temperature (°C)	Refs.
Acid with fluorine	HF	Room temperature to 55	[49]
	$H_2O_2 + HF$	40	[50]
	HCl + LiF	35–55	[51]
	HCl + (Na, K, or NH_4F)	30–60	[52]
	NH_4HF_2	Room temperature	[53]
Molten salts	LiF + NaF + KF	550	[54]
Hydrothermal	NaOH	270	[55]
	$NaBF_4$, HCl	180	[56]
Electrochemical	NH_4Cl/TMAOH	Room temperature	[57]
	HCl	Room temperature	[58]
Lewis acid	$ZnCl_2$	550	[59]

ers, like Cr_2N and Mn_2C, are antiferromagnetic [60]. They have been used as electromagnetic shielding materials [64] and have found their way into bioimaging [36]. Furthermore, MXenes find their application as catalysts [65,66], energy storage [67], theranostic nanomedicines [68], supercapacitors [69], and even reinforcing agents [70].

3. Electrospun MXenes/nanofiber composites for biomedical application

Electrospun nanofibers are already used for tissue engineering applications due to their resemblance with the extracellular matrix of the human body [71]. Fabrication of biologically functional nanofibers while introducing tissue enhancers in natural and synthetic polymers has shown promising results [72]. Researchers have worked on improvising the properties by introducing additional moieties such as graphene [73], metallic [74], and non-metallic nanoparticles [75], different drugs [76], and many more. All these composite nanofibers containing various enhancers have resulted in more advanced applications than their pristine counterpart. Likewise, after discovering MXenes, researchers have tried to incorporate this new material into the nanofibers and tested their biomedical applications. The results obtained have been remarkable and are discussed in the later sections. However, only a little work has been achieved so far where nanofibers are modified with MXenes to improve their efficiency towards biomedical use. In this regard, one of the initial works has been performed by Mayerberger *et al.*, in which they have electrospun poly(acrylic acid), polyethylene oxide, poly(vinyl alcohol), and alginate/polyethylene oxide incorporated with 1 wt% of Ti_3C_2 nano-flakes [77]. They have shown that single-layer $Ti_3C_2T_x$ suspensions can be directly formed into nanofibers using the polymers mentioned above, and these nano-flakes are well-dispersed during the electrospinning. The result revealed using a small amount of Ti_3C_2 flakes could successfully affect the crystal structure of polyethylene oxide nanofibers. Its unique mechanical and electrical properties open a new door for fabricating MXenes/nanofibers with tuneable characteristics and applications.

3.1. MXenes/nanofiber composite for bone regeneration and antimicrobial activity

Currently, for biomedical applications, polymer-functionalized MXenes, have been used for their antibacterial [78], photothermal treatment [79], drug administration [33], biosensors [80], and bone regeneration [81] due to their 2D planar structure, which outshines them with best characteristics [82]. For synthesizing Ti_3C_2 MXenes, hydrofluoric acid etching was performed, and then these nano-flakes were dispersed in a poly(ε-caprolactone) solution and formed into nanofibers by electrospinning [83]. The results indicated that 26.07% calcium and 17.15% phosphate were passively deposited, which was attributed due to the better wettability of MXenes, and acting as the site of induction of crystal formation (Fig. 4a). Fibroblast's (NIH-3T3) viability on the 5th day of culture was almost 70% confluent than the control. Moreover, for poly(ε-caprolactone)-MXene composite (0.2 and 0.5 wt%), pre-osteoblasts (MC3T3-E1) viability was higher (*i.e.*, 72%) than fibroblasts. This may indicate when Ti_3C_2 MXenes are incorporated into poly(ε-caprolactone) nanofibers that can be suitable candidates for bone implants.

In another approach, antimicrobial material was fabricated by electrospinning. Here encapsulated $Ti_3C_2T_z$ MXene was introduced in chitosan nanofibers [84]. The $Ti_3C_2T_z$/chitosan composite nanofibers were tested for antibacterial activity using *Escherichia coli* and *Staphylococcus aureus.* The results showed a 95% and 62% sharp decline in colony-forming units, respectively, after 4 h of treatment with the 0.75 wt% $Ti_3C_2T_z$-loaded nanofibers. According to the author, increased antibacterial activity was seen in the nanofibers, which were crosslinked with the glutaraldehyde; bacterial viability results can be seen in Fig. 4b. The rationale for the antibacterial property was because of the penetration of these nano-flakes causing distorted morphology to bacteria (Fig. 4b, scanning electron microscope (SEM) images). However, the authors could not ascertain the exact mechanism for the antibacterial properties of $Ti_3C_2T_z$. Furthermore, the cytotoxicity test was conducted using HeLa cells to examine the material's biocompatibility. At all test concentrations, the average cell viabilities were greater than 85% compared to the control for 72 h, demonstrating that the mats are not cytotoxic using the alamarBlue® assay.

Using antibacterial agents in the electrospun fibers and allowing them to release upon specific responses is one of the ways to impart the bactericidal activity in nanofibers [85]. Similarly, amoxicillin release upon heat response due to MXene has imparted antibacterial activity in poly(vinyl alcohol) nanofibers. In one of the

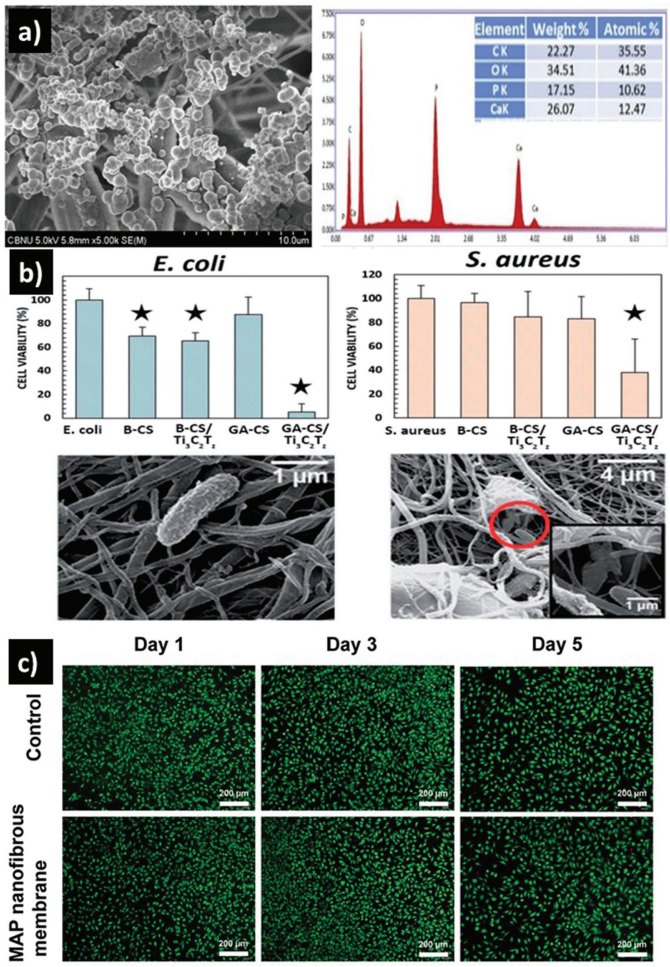

Fig. 4. Representation of results obtained for the different MXenes/polymer nanofiber composite for biomedical application: (a) SEM image with energy-dispersive X-ray spectroscopy (EDS) of biomineralization of MXene-poly(ε-caprolactone) (PCL) composite fibers, (b) SEM image along with a bar graph representation of the antimicrobial activity of $Ti_3C_2T_z$ (MXene) flakes within chitosan nanofibers, (c) phase-contrast images for cellular viability of L929 (mouse fibroblast) cells for MXene, amoxicillin, and poly(vinyl alcohol) (MAP) nanofibers. (B, basified with NaOH; CS, chitosan; GA, crosslinked with glutaraldehyde). Reproduced with permission [83]. Copyright 2020, Elsevier B.V.; Reproduced with permission [84]. Copyright 2018, The Royal Society of Chemistry; Reproduced with permission [86]. Copyright 2021, Elsevier B.V.

works, a synergistically developed localized hyperthermia by exposure of near-infrared laser to MXene when embedded in the poly(vinyl alcohol) nanofibers, which were simultaneously loaded with amoxicillin [86]. After performing the cross-linking by glutaraldehyde vapors, the fibers turned insoluble in the water. The inclusion of MXene was to encourage the release of amoxicillin as MXene could convert the near-infrared laser into heat, causing localized hyperthermia, likewise highly oxidized ilmenite nanosheets created local hypothermia at 808 nm laser for photo-thermal therapy [87]. It was calculated that introducing MXene led to 41.9% efficiency in photothermal activity, which promoted the release of amoxicillin. Further, the hemolytic treatment showed 1.7% haptoglobin upon lysis which is comparatively lower than the critical value (5%), indicating hemocompatibility of these fabricated nanofibers. As for the antibacterial activity, it was observed that the bactericidal effect could be reached up to 96.1% for *Escherichia coli* and 99.1% for *Staphylococcus aureus*. Moreover, for biocompatibility, L929 (mouse fibroblast) cells were cultured in DMEM as control alongside MXene, amoxicillin, and poly(vinyl alcohol) nanofibers, resulting in >90% survival rate of cells, as can be observed in Fig. 4c.

3.2. MXenes/nanofiber composite for cellular differentiation

Due to their exceptional characteristics, MXenes are promising materials for various applications. However, very little research on how MXene affects cell division and proliferation is conducted. In this regard, one such biomaterial has been fabricated using Ti_3C_2 MXene composite nanofibers [88]. Herein, electrospinning was used to create the composite nanofibers using poly(L-lactide)-polyhydroxyalkanoates with Ti_3C_2. The resultant material showed comparatively good hydrophilicity. Later, these MXenes nanosheets were also dip-doped onto these mats, further increasing the hydrophilicity and providing adequate functional elements for cellular proliferation. Fig. 5a shows SEM image of bone marrow-derived mesenchymal stem cells attached to the MXene-modified nanofiber. Fig. 5b shows a transmission electron microscope (TEM) image indicating the presence of MXene nanoparticles. The MTT (3-[4,5-dimethylthiazol-2-yl]-2,5 diphenyl tetrazolium bromide) results showed increased growth than the untreated nanofiber during different culture times (Fig. 5c). Moreover, MXene composite nanofibers offered favorable cellular development and differentiation microenvironment. The results indicated more than a unit-fold change in osteogenic-related genes (*Colla1*, *OCN*, *OPN*, *RUNX2*) for cells cultured on MXene-modified nanofibers (Fig. 5d). Further, doped MXenes also led to a decent cellular spread than its counterpart. Moreover, these mats provided a good platform for cellular proliferation. Similarly, MXenes were used to promote osteodifferentiation [89]. Herein, MXenes were decorated on poly(L-lactide-*co*-ε-caprolactone)/collagen-based nanofibers. The modified fibers showed comparatively low contact angle measurements concerning the pristine nanofiber mat. It was observed that fabricated nanofiber had good physicochemical characteristics and physical similarities with the natural extracellular matrix, which created favorable microenvironments for differentiation for MC3T3-E1 pre-osteoblasts. Moreover, the author concluded that the topography of MXene-decorated nanofiber also favored the differentiation process. The results also revealed that there was a significant increase in alkaline phosphatase activity (which indicates the existence of osteoblasts and the development of new bone) at 20 μg/mL of MXene-modified nanofiber mats when cultured for 14 days; the results can be observed in Fig. 5e along with Fig. 5f which put forward Von Kossa-stained samples indicating mineralization due to cellular differentiation.

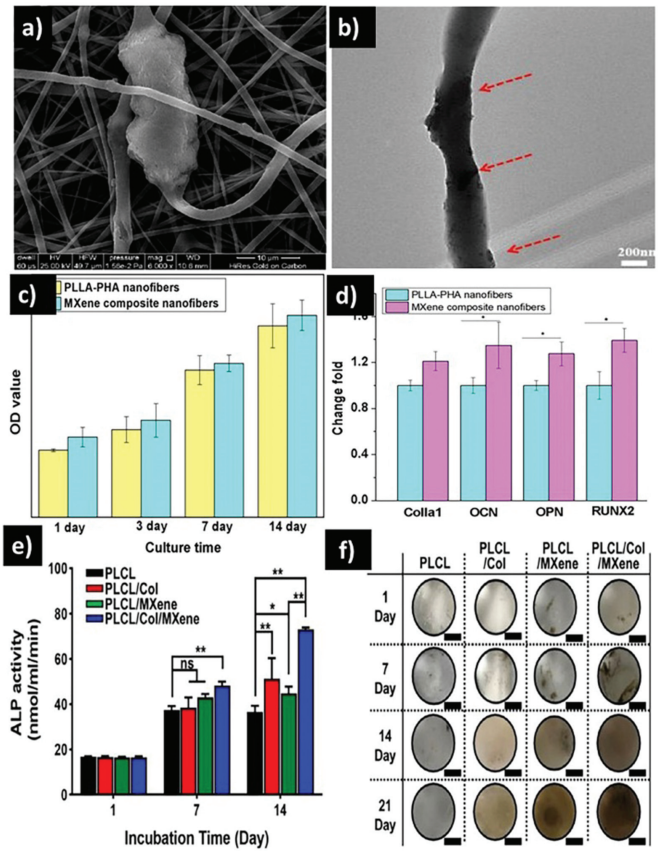

Fig. 5. Representation of data illustrating MXenes/polymer composite for cellular differentiation: (a) SEM image of BMSCs on PLLA-PHA nanofibers, (b) TEM image of fiber (arrows indicate the presence of MXenes in the fiber), (c) bar graph representation of results obtained from MTT assay, (d) bar graph showing results for osteogenic primers present after 14 days culture, (e) ALP activity for showing the presence of MC3T3-E1 pre-osteoblast cells on PLCL, PLCL/Col, PLCL/MXene, PLCL/Col/MXene nanofibrous, and (f) Von Kossa-stained samples indicating mineralization due to cellular differentiation. (BMSC, bone marrow-derived mesenchymal stem cell; PLLA, poly(L-lactide); PLCL, poly(L-lactide-*co*-ε-caprolactone); Col, collagen). Reproduced with permission [88]. Copyright 2020, American Chemical Society; Reproduced with permission [89]. Copyright 2022, The Author(s).

3.3. MXenes/nanofiber composite for wound healing

The best materials for wound repair are emerging scaffolds made of nanofibers because they have more outstanding cell attachment properties, drug loading, and friendly interactions with the wound interface. However, their application in biomedical fields is constrained even though they support many therapeutic effects. They only offer the random release of active components and cannot establish long-term and stable control release for wound sites. In this regard, the controlled release of vitamin E from heat-responsive polymer/MXene nanobelt fibers has been reported [90]. Herein, polyacrylonitrile and polyvinylpyrrolidone, along with MXenes, were used. An additional layer of heat-sensitive PAAV (co-polymer) was also added, which led to the release of loaded material upon heat produced by the photothermal effect caused by MXene. The schematic representation and the obtained morphology are shown in Fig. 6a. The developed MXene composite nanofiber produces heat when exposed to NIR; the temperature rose quickly to 60 °C in 120 s. It was observed that altering the near-infrared (NIR) light changed the temperature values. For 0.5 W power, the temperature rise was 42 °C when exposed to the 180 s. Meanwhile, 0.33 W was used as a safe level for practical application leading to a 42 °C temperature rise for 180 s. The author states that MXenes helped in releasing the antibi-

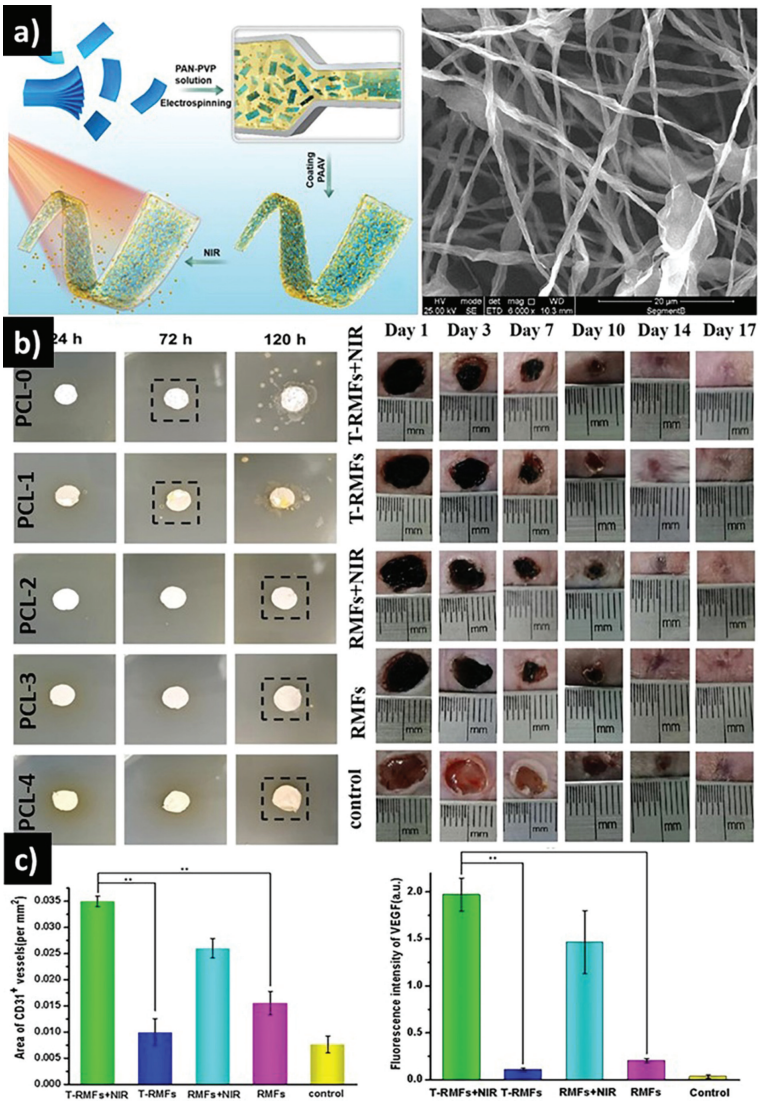

Fig. 6. Illustration of Mxene incorporated in polymer and representation of data showing wound healing ability for the fabricated composite: (a) general schematics of MXene/nanofiber along with SEM, (b) images showing antimicrobial (left) and wound healing (right) capability of the fabricated material, (c) immunohistochemical study showing elevated CD31 expression. (PCL-0, 100% poly(ε-caprolactone); PCL-1, 97% poly(ε-caprolactone) and 3% $Ti_3C_2T_x$; PCL-2, 97% poly(ε-caprolactone) and 3% baicalin; PCL-3, 94% poly(ε-caprolactone), 3% $Ti_3C_2T_x$ and 3% baicalin; PCL-4, 92% poly(ε-caprolactone) 3% $Ti_3C_2T_x$ and 5% baicalin). Reproduced with permission [90]. Copyright 2021, The Author(s); Reproduced with permission [91]. Copyright 2022, The Author(s).

otic and led to enhanced antibacterial activity, as shown in Fig. 6b (left panel). Moreover, the change in temperature attributes stability along with the long-term release of vitamin E, which later increases wound healing. The results revealed mats containing MXenes/vitamin E/thermosensitive polymer resulted in complete wound recovery within 17 days (Fig. 6b, right panel); moreover, the quantitative analysis was accessed by hematoxylin-eosin staining. In addition to providing sound photothermal effects, the MXene nanosheets within these materials also offered functional groups for cell development, which was reported using immunohistochemical studies. The studies showed significant angiogenesis and elevated CD31 expression, as shown in Fig. 6c. It was also observed that there was a substantial rise in blood vessels for wounds treated with NIR-exposed nanofibers containing vitamin E. This allowed suitable availability of nutrients and oxygen for better wound healing properties of nanofiber mat. In one of the works, MXenes, along with baicalin (antibiotic) loaded in nanofiber, have been fabricated and tested as antibacterial wound dressing material [91]. A synergistic effect of $Ti_3C_2T_x$ nano-flakes and baicalin in poly(ε-caprolactone) nanofibers exhibited significant antibacterial activity against the *Staphylococcus aureus*. The results revealed a substantial decrease in contact angle from 127.1° to 65.5° upon the addition of MXenes and baicalin due to the presence of OH groups, as reported by the author. The material to be used for wound healing should inherit antibacterial activity to take care of infections. For that purpose, baicalin (poorly insoluble in water) should be released from the nanofiber adequately. Further, these materials showed good biocompatibility.

3.4. MXenes/nanofiber composite for neural tissue engineering

Further, being electrically active, MXenes also find their application into neural tissue regeneration. Deploying artificial channels as bridges to encourage the development of regenerating nerves and assist them through the injured area is necessary to restore neuronal damage. However, various natural and synthetic polymers have been used for neural tissue engineering [92]. Likewise, poly(3,4-ethylene dioxythiophene) holds good biocompatibility and adequate electrical and chemical stability; however, its chronic inflammatory effect and low degradative nature make it an unwor-

thy candidate. Currently, MXenes have been used as additives to polymeric nanofibers, which are employed to grow supporting cells and give them sustaining neurotrophic qualities [93]. Herein, MXene modification of polylactic acid nanofibers was performed to validate the requirements for nerve-guiding path formation. The introduction of MXenes increased the electrical conductivity of the material. The current flow in the modified nanofiber membrane was <150 mA for an applied voltage of 5.5 V. However, higher potential resulted in the dielectric behavior of fabricated nanofiber. These findings demonstrate that MXenes can be used to make polymer membranes electroconductive for neural tissue engineering applications. The presence of polylactic acid membranes containing immobilized MXenes did not appear to have any adverse effects on the cells, according to the resazurin reduction experiment. However, the results were only partially satisfying due to improper immobilization of MXenes and improper handling during cell culture. Further, the material also exhibited the potential to prevent bacterial adhesion due to MXenes in the system, resulting in destroying cell shape and cellular membrane. These properties open new doors for using MXenes-polymer composite in creating neural guidance conduits.

4. Conclusion

The use of MXenes in nanofibers has laid the foundation for a new class of materials tested for various biological and non-biological applications. The properties such as biocompatibility, mechanical stability, thermal activity, and low toxicity have been attributed to their potential use in the biomedical field. Using them with nanofibers has further enhanced their role in the biomedical field. As discussed above, these composites directly affect antibacterial activity, cellular differentiation, wound healing ability, and neural tissue regeneration. Using different MXenes as a filler in the various nanofibers can further help to exploit their properties in the biomedical field. In addition, these materials find their indirect biological application, such as self-powered tribo/piezoelectric nanogenerators [94,95]. Although very little has been done in this regard, seeing the essence of this modification tool, it was necessary to put forward this communication, using MXenes and encasing them in nanofibers for biomedical applications. It is pertinent to mention that most of the work has been achieved using titanium carbide MXenes in the nanofibers. However, more than 20 different MXenes still need to be tested for their biomedical application when used as filler inside the nanofiber. Moreover, MXenes synthesis often involves toxic and corrosive liquids, which can undesired biomedical applications and can have an environmental impact. Hopefully, this review will open a new way to modify more nanofibers with new MXenes and account for their biomedical application.

Declaration of competing interest

The authors declare that they have no known competing financial interests or personal relationships that could have appeared to influence the work reported in this paper.

Acknowledgment

This work was supported by the research grants received by Dr. Faheem A. Sheikh from Science and Engineering Research Board (SERB) (No. CRG/220/000113).

References

[1] D.F. Ogletree, P.J. Schuck, A.F. Weber-Bargioni, et al., Adv. Mater. 27 (2015) 5693–5719.
[2] G. Ramalingam, P. Kathirgamanathan, G. Ravi, et al., *Quantum confinement effect of 2D nanomaterials*, in: F. Divsar (Ed.), Quantum Dots—Fundamental and Applications, IntechOpen, London, 2020, pp. 11-19.
[3] J. Zhou, L. Shen, M.D. Costa, et al., Sci. Data 6 (2019) 86.
[4] Y. Dong, Z.S. Wu, W. Ren, H.M. Cheng, X. Bao, Sci. Bull. (Beijing) 62 (2017) 724–740.
[5] K. Zhang, Y. Feng, F. Wang, Z. Yang, J. Wang, J. Mater. Chem. C 5 (2017) 11992–12022.
[6] C. Ataca, H. Sahin, S. Ciraci, J. Phys. Chem. C 116 (2012) 8983–8999.
[7] R. Irshad, K. Tahir, B. Li, et al., J. Indust. Eng. Chem. 64 (2018) 60–69.
[8] A. Kara, H. Enriquez, A.P. Seitsonen, et al., Surf. Sci. Rep. 67 (2012) 1–18.
[9] C. Hou, G. Tai, Z. Wu, J. Hao, ChemPlusChem 85 (2020) 2186–2196.
[10] P. Ares, K.S. Novoselov, Nano Mater. Sci. 4 (2022) 3–9.
[11] A.K. Geim, K.S. Novoselov, The rise of graphene, in: P. Rodgers (Ed.), Nanoscience and Technology: A Collection of Reviews from Nature Journals, World Scientific Publishing Company, Singapore, 2009, pp. 11–19.
[12] G. Reina, J.M. González-Domínguez, A. Criado, et al., Chem. Soc. Rev. 46 (2017) 4400–4416.
[13] M. Pourmadadi, A. Tajiki, S.M. Hosseini, et al., J. Drug Deliv. Sci. Technol. 76 (2022) 103767.
[14] M. Ou, X. Wang, L. Yu, et al., Adv. Sci. 8 (2021) 2001801.
[15] T. Chen, W. Zeng, C. Tie, et al., Bioact. Mater. 10 (2022) 515–525.
[16] R. Mas-Balleste, C. Gomez-Navarro, J. Gomez-Herrero, F.J.N. Zamora, Nanoscale 3 (2011) 20–30.
[17] Y. Gogotsi, B. Anasori, ACS Nano 13 (2019) 8491–8494.
[18] A. Eatemadi, H. Daraee, N. Zarghami, et al., Artif. Cells Nanomed. Biotechnol. 44 (2016) 111–121.
[19] J. Xue, T. Wu, Y. Dai, Y Xia, Chem. Rev. 119 (2019) 5298–5415.
[20] N. Bhardwaj, S.C. Kundu, Biotechnol. Adv. 28 (2010) 325–347.
[21] D. Zhao, T. Zhu, J. Li, et al., Bioact. Mater. 6 (2021) 346–360.
[22] X. Zhang, W. Qu, D. Li, et al., Adv. Mater. Interfaces 7 (2020) 2000225.
[23] J. Zhang, X. Zhang, C. Wang, et al., Adv. Healthc. Mater. 10 (2021) 2000604.
[24] R. Pasricha, D. Sachdev, Biological characterization of nanofiber composites, in: M. Ramalingam, S. Ramakrishna (Eds.), Nanofiber Composites for Biomedical Applications, Woodhead Publishing, Elsevier, Cambridge, 2017, pp. 157–196.
[25] Z. Liu, J. Zhang, C. Fu, J. Ding, Asian J. Pharm. Sci. 18 (2023) 100774.
[26] K. Liu, L. Yan, R. Li, et al., Adv. Sci. 9 (2022) 2103875.
[27] S. Bahrami, A. Solouk, H. Mirzadeh, A.M. Seifalian, Composites Part B: Eng 168 (2019) 421–431.
[28] P. Ahmadi, N. Nazeri, M.A. Derakhshan, H. Ghanbari, Int. J. Biol. Macromol. 180 (2021) 590–598.
[29] X. Ma, G. Wu, F. Dai, et al., Carbohydr. Polym. 251 (2021) 117058.
[30] A.H. Rather, R.S. Khan, T.U. Wani, et al., Int. J. Biol. Macromol. 226 (2022) 690–705.
[31] A.H. Rather, T.U. Wani, R.S. Khan, et al., Int. J. Mol. Sci. 22 (2021) 4017.
[32] H.S. Sofi, T. Akram, A.H. Tamboli, et al., Int. J. Pharm. 569 (2019) 118590.
[33] N. Rabiee, M. Bagherzadeh, M. Jouyandeh, et al., ACS Appl. Bio Mater. 4 (2021) 5106–5121.
[34] S. Iravani, R.S. Varma, Mater. Adv. 2 (2021) 2906–2917.
[35] M. Malaki, R.S. Varma, Adv. Mater. 32 (2020) 2003154.
[36] M. Huang, Z. Gu, J. Zhang, et al., J. Mater. Chem. B 9 (2021) 5195–5220.
[37] A. Sundaram, J.S. Ponraj, C. Wang, et al., J. Mater. Chem. B 8 (2020) 4990–5013.
[38] Y. Zhong, S. Huang, Z. Feng, Y. Fu, A. Mo, J. Biomed. Mater. Res. 110 (2022) 1840–1859.
[39] I. Mahar, F.H. Memon, J.W. Lee, et al., Membranes 11 (2021) 869.
[40] V. Chaudhary, V. Khanna, H.T.A. Awan, et al., Biosens. Bioelectron. 220 (2023) 114847.
[41] A. Zhou, Y. Liu, S. Li, et al., J. Adv. Ceram. 10 (2021) 1194–1242.
[42] M. Naguib, Y. Gogotsi, Acc. Chem. Res. 48 (2015) 128–135.
[43] P. Istomin, E. Istomina, A. Nadutkin, et al., Ceram. Int. 43 (2017) 16128–16135.
[44] O. Salim, K.A. Mahmoud, K.K. Pant, R.K. Joshi, Mater. Today Chem. 14 (2019) 100191.
[45] M. Naguib, O. Mashtalir, J. Carle, et al., ACS Nano 6 (2012) 1322–1331.
[46] K.R.G. Lim, M. Shekhirev, B.C. Wyatt, et al., Nat. Synth. 1 (2022) 601–614.
[47] J. Halim, S. Kota, M.R. Lukatskaya, et al., Adv. Funct. Mater. 26 (2016) 3118–3127.
[48] L. Verger, V. Natu, M. Carey, M.W. Barsoum, Trends Chem 1 (2019) 656–669.
[49] M. Naguib, M. Kurtoglu, V. Presser, et al., Adv. Mater. 23 (2011) 4248–4253.
[50] M. Alhabeb, K. Maleski, T.S. Mathis, et al., Angew. Chem. 130 (2018) 5542–5546.
[51] M. Ghidiu, M.R. Lukatskaya, M.Q. Zhao, Y. Gogotsi, M.W. Barsoum, Nature 516 (2014) 78–81.
[52] F. Liu, A. Zhou, J. Chen, et al., Appl. Surf. Sci. 416 (2017) 781–789.
[53] L.H. Karlsson, J. Birch, J. Halim, M.W. Barsoum, P.O.A. Persson, Nano Lett 15 (2015) 4955–4960.
[54] P. Urbankowski, B. Anasori, T. Makaryan, et al., Nanoscale 8 (2016) 11385–11391.
[55] T. Li, L. Yao, Q. Liu, et al., Angew. Chem. 57 (2018) 6115–6119.
[56] C. Peng, P. Wei, X. Chen, et al., Ceram. Int. 44 (2018) 18886–18893.
[57] S. Yang, P. Zhang, F. Wang, et al., Angew. Chem. 130 (2018) 15717–15721.
[58] W. Sun, S. Shah, Y. Chen, et al., J. Mater. Chem. A 5 (2017) 21663–21668.
[59] M. Li, J. Lu, K. Luo, et al., J. Am. Chem. Soc. 141 (2019) 4730–4737.
[60] X. Zhan, C. Si, J. Zhou, Z. Sun, Nanoscale Horiz 5 (2020) 235–258.
[61] J. Cao, Z. Zhou, Q. Song, et al., ACS Nano 14 (2020) 7055–7065.
[62] S.M.S. Rana, M.T. Rahman, M. Salauddin, et al., ACS Appl. Mater. Interfaces 13 (2021) 4955–4967.

[63] R. Rajeev, D.A. Thadathil, A. Varghese, Crit. Rev. Solid State Mater. Sci. (2022) 1–43.
[64] A. Iqbal, P. Sambyal, C.M. Koo, Adv. Funct. Mater. 30 (2020) 2000883.
[65] J. Sun, W. Kong, Z. Jin, et al., Chin. Chem. Lett. 31 (2020) 953–960.
[66] J. Yin, F. Zhan, T. Jiao, et al., Chin. Chem. Lett. 31 (2020) 992–995.
[67] Z. Bao, C. Lu, X. Cao, et al., Chin. Chem. Lett. 32 (2021) 2648–2658.
[68] Y. Wang, W. Feng, Y. Chen, Chin. Chem. Lett. 31 (2020) 937–946.
[69] H. He, Q. Xia, B. Wang, et al., Chin. Chem. Lett. 31 (2020) 984–987.
[70] J. Hu, S. Li, J. Zhang, et al., Chin. Chem. Lett. 31 (2020) 996–999.
[71] M. Keshvardoostchokami, S.S. Majidi, P. Huo, et al., Nanomaterials 11 (2020) 21.
[72] N. Udomluck, W.G. Koh, D.J. Lim, H. Park, Int. J. Mol. Sci. 21 (2019) 99.
[73] A. Fakhrali, M. Nasari, N. Poursharifi, et al., J. Appl. Polym. Sci. 138 (2021) 51177.
[74] D.N. Phan, N. Dorjjugder, M.Q. Khan, et al., Cellulose 26 (2019) 6629–6640.
[75] K.E. Mosaad, K.R. Shoueir, A.H. Saied, M.M. Dewidar, Ann. Biomed. Eng. 49 (2021) 2006–2029.
[76] R.S. Bhattarai, R.D. Bachu, S.H. Boddu, S. Bhaduri, Pharmaceutics 11 (2018) 5.
[77] E.A. Mayerberger, O. Urbanek, R.M. McDaniel, et al., J. Appl. Polym. Sci. 134 (2017) 45295.
[78] K. Rasool, K.A. Mahmoud, D.J. Johnson, et al., Sci. Rep. 7 (2017) 1598.
[79] L. Yang, S. Chen, H. Wei, et al., ACS Appl. Mater. Interfaces 14 (2022) 45178–45188.
[80] T.M. Kim, B. Ryplida, G. Lee, S.Y. Park, E. Chemistry, J. Ind. Eng. Chem. 120 (2022) 188–194.
[81] K. Chen, Y. Chen, Q. Deng, et al., Mater. Lett. 229 (2018) 114–117.
[82] S.M. George, B. Kandasubramanian, Ceram. Int. 46 (2020) 8522–8535.
[83] G.P. Awasthi, B. Maharjan, S. Shrestha, et al., Colloids Surf. A 586 (2020) 124282.
[84] E.A. Mayerberger, RM. Street, RM. McDaniel, MW. Barsoum, C.L. Schauer, RSC Adv. 8 (2018) 35386–35394.
[85] J. Zhang, C. Xiao, X. Zhang, et al., J. Control. Release 335 (2021) 359–368.
[86] X. Xu, S. Wang, H. Wu, et al., Colloids Surf. B 207 (2021) 111979.
[87] M. Ou, C. Pan, Y. Yu, et al., Chem. Eng. J. 390 (2020) 124524.
[88] R. Huang, X. Chen, Y. Dong, et al., ACS Appl. Bio Mater. 3 (2020) 2125–2131.
[89] S.H. Lee, S. Jeon, X. Qu, et al., Nano Converg. 9 (2022) 38.
[90] L. Jin, X. Guo, D. Gao, et al., NPG Asia Mater. 13 (2021) 24.
[91] W. Zeng, N. Cheng, X. Liang, et al., Sci. Rep. 12 (2022) 10900.
[92] S. Amini, H. Salehi, M. Setayeshmehr, M. Ghorbani, Polym. Adv. Technol. 32 (2021) 2267–2289.
[93] S. Kyrylenko, V. Kornienko, O. Gogotsi, et al., Proceedings of the IEEE 10th international conference nanomaterials: applications & properties (NAP), 2020.
[94] S. Wang, H.Q. Shao, Y. Liu, et al., Compos. Sci. Technol. 202 (2021) 108600.
[95] H. Xu, X. Wang, J. Niu, et al., Adv. Mater. Interfaces 9 (2022) 2102085.